

		Volume 28 Number 18 30 October 2008 ISSN 0278-4343
		<h1>CONTINENTAL SHELF RESEARCH</h1>
Editors: Michael Collins Southampton, UK Richard W. Sternberg Seattle, WA, USA		
Research Papers		
R.J.K. Dunn, D.T. Welsh, P.R. Teasdale, S.Y. Lee, C.J. Lemckert and T. Meziane	2535	Investigating the distribution and sources of organic matter in surface sediment of Coombabah Lake (Australia) using elemental, isotopic and fatty acid biomarkers
F. Donda, E. Gordini, M. Rebecco, V. Pascucci, G. Fontolan, P. Lazzari and R. Mosetti	2550	Shallow water sea-floor morphologies around Asinara Island (NW Sardinia, Italy)
L. Zhong, M. Li and M.G.G. Foreman	2565	Resonance and sea level variability in Chesapeake Bay
C. Sassa, Y. Tsukamoto, K. Nishiuchi and Y. Konishi	2574	Spawning ground and larval transport processes of jack mackerel <i>Trachurus japonicus</i> in the shelf-break region of the southern East China Sea
R.F. Shipe, A. Leinweber and N. Gruber	2584	Abiotic controls of potentially harmful algal blooms in Santa Monica Bay, California
G.E. Sánchez, S. Pantoja, C.B. Lange, H.E. González and G. Daneri	2594	Seasonal changes in particulate biogenic and lithogenic silica in the upwelling system off Concepción (~36°S), Chile, and their relationship to fluctuations in marine productivity and continental input
A. Silva, S. Palma and M.T. Moita	2601	Coccolithophores in the upwelling waters of Portugal: Four years of weekly distribution in Lisbon bay
www.elsevier.com/locate/csr		

This article appeared in a journal published by Elsevier. The attached copy is furnished to the author for internal non-commercial research and education use, including for instruction at the authors institution and sharing with colleagues.

Other uses, including reproduction and distribution, or selling or licensing copies, or posting to personal, institutional or third party websites are prohibited.

In most cases authors are permitted to post their version of the article (e.g. in Word or Tex form) to their personal website or institutional repository. Authors requiring further information regarding Elsevier's archiving and manuscript policies are encouraged to visit:

<http://www.elsevier.com/copyright>



Contents lists available at ScienceDirect

Continental Shelf Research

journal homepage: www.elsevier.com/locate/csr

Resonance and sea level variability in Chesapeake Bay

Liejun Zhong^{a,*}, Ming Li^a, M.G.G. Foreman^b^a Horn Point Laboratory, University of Maryland Center for Environmental Science, P.O. Box 775, Cambridge, MD 21613, USA^b Institute of Ocean Sciences, Fisheries and Oceans Canada, P.O. Box 6000, Sidney, British Columbia, Canada V8L 4B2

ARTICLE INFO

Article history:

Received 12 October 2007

Received in revised form

25 May 2008

Accepted 16 July 2008

Available online 30 July 2008

Keywords:

Tidal resonance

Sea level variability

Numerical modeling

Chesapeake Bay

ABSTRACT

A numerical model is used to determine the resonant period and quality factor Q of Chesapeake Bay and explore physical mechanisms controlling the resonance response in semi-enclosed seas. At the resonant period of 2 days, the mouth-to-head amplitude gain is 1.42 and Q is 0.9, indicating that Chesapeake Bay is a highly dissipative system. The modest amplitude gain results from strong frictional dissipation in shallow water. It is found that the spatial distribution of energy dissipation varies with forcing frequency. While energy at tidal frequencies is dissipated around topographic hotspots distributed throughout the Bay, energy dissipation at subtidal frequencies is mainly concentrated in the shallow-water lower Bay. An analytic calculation shows that the bottom friction parameter is much larger in Chesapeake Bay than in other coastal systems with strong resonance response. The model-predicted amplitude gains and phase changes agree well with the observations at semidiurnal and diurnal tidal frequencies. However, the predicted amplitude gain in the resonant frequency band (34–54 h period) falls below that inferred from band-passed sea level observations. This discrepancy can be attributed to the local wind forcing which amplifies the sea level response in the upper Bay. The model is also used to show that rising sea levels associated with global warming will shift the resonance period of Chesapeake Bay closer to the diurnal tides and thus exacerbate flooding problems by causing an increase in tidal ranges.

© 2008 Elsevier Ltd. All rights reserved.

1. Introduction

The response of semi-enclosed seas or bays to offshore sea level fluctuations depends on a number of factors including the magnitude and frequency of offshore forcing, the details of water depth and coastline, and the strength of friction. A resonance response can be excited if the natural resonance frequency of the semi-enclosed sea is close to one of the forcing frequencies at the offshore boundary. For example, the Bay of Fundy and Gulf of California have natural resonance periods which are close to those for semidiurnal or diurnal tides. In these bays the semidiurnal or diurnal tide at the head is greatly amplified as compared to that at the mouth. In the shallow Long Island Sound, the semidiurnal tides experience a fourfold amplification due to resonance (Wong, 1990). In contrast, the amplification in the Jude de Fuca and Strait of Georgia is only 20%. What is the main factor controlling the resonance response in semi-enclosed seas? Is it the distance between the resonance frequency and forcing frequency or the strength of bottom friction? If the resonance frequency is lower

than the diurnal and semidiurnal tidal frequencies, can wind-induced sea level fluctuations over the open shelf excite strong resonance responses inside the semi-enclosed bay?

Analytic and numerical models have been developed to calculate the resonant frequency and quality factor/dissipation parameter Q in semi-enclosed seas and other coastal oceans. Garrett (1972) determined the period of free-mode oscillation in the Bay of Fundy and Gulf of Maine to be 13.3 h with $Q = 5.25$ and proposed that the lunar M_2 tide in the North Atlantic produces the resonance response and the unusually high tides in the area. Using a finite element, barotropic, tidal model, Foreman et al. (1993) estimated the resonant period of the north coast of British Columbia to be 7.6 h with $Q = 9.5$. Similarly, Carbajal and Backhaus (1998) examined the wave energy flux into the Gulf of California and found resonant periods at 14.57, 6.25 h, etc. and a high value of $Q = 18.8$. In a recent paper, Sutherland et al. (2005) used the observed tidal elevation gain and phase change from the Pacific Ocean through Juan de Fuca Strait and into the Strait of Georgia, to fit the predictions of simple analytic models, and found a resonant period of 17–21 h and Q of only 2 for this coastal system. They pointed out that the low Q value is an indication that the Juan de Fuca Strait and Strait of Georgia system is a highly dissipative system. What makes Fuca–Georgia system more dissipative than the other systems that experience a much stronger resonance response?

* Current address: CSIRO Marine and Atmospheric Research, Underwood Ave., Floreat, WA 6014, Australia. Tel.: +61 8 9333 6533; fax: +61 8 9333 6555.

E-mail address: Liejun.Zhong@csiro.au (L. Zhong).

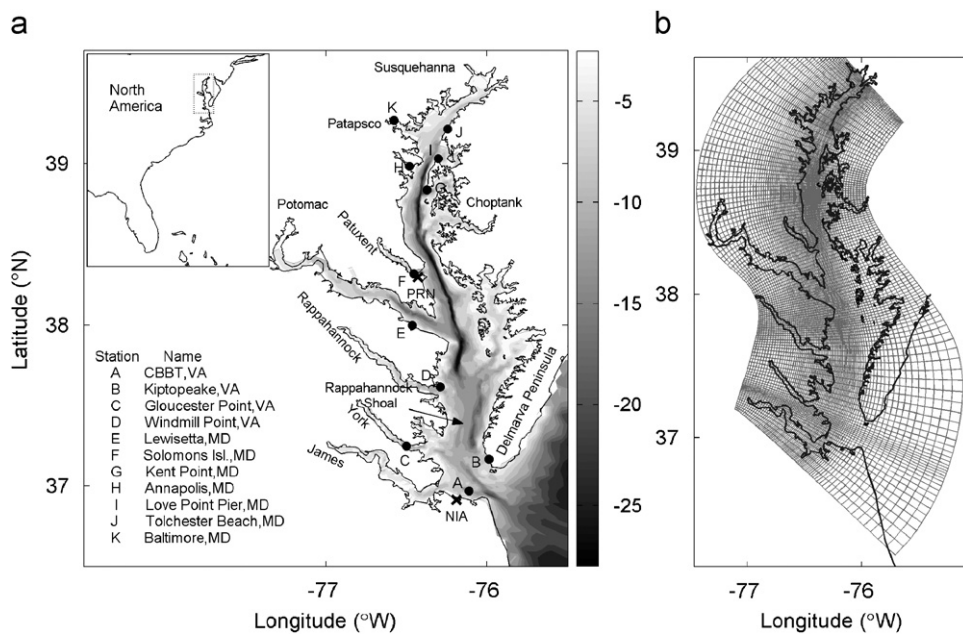


Fig. 1. (a) Map of Chesapeake Bay bathymetry (depths are in meters), tidal gauge stations (dots) and wind stations (crosses) of Norfolk International Airport (NIA) and Patuxent River Naval station (PRN) with an insert showing the location of Chesapeake Bay in the North America, and (b) the horizontal curvilinear coordinate system for the numerical model.

Using Chesapeake Bay as an example, we shall further explore the physics of energy dissipation in semi-enclosed seas. Chesapeake Bay is a semi-enclosed Bay and partially mixed estuary, consisting of a long main stem interacting with a number of tributaries arrayed along its axis (Fig. 1(a)). The main stem stretches for about 320 km from the mouth of the Susquehanna River at Havre de Grace, Maryland to the seaward end at Cape Charles and Cape Henry, Virginia. It is shallow, with a mean water depth of 6.5 m. However, a deep paleochannel running in the north–south direction dominates the bathymetry in the middle reaches of the main Bay. Tides in Chesapeake Bay are modest with the maximum range of about 1 m and show no significant amplification between the mouth and head. This suggests that Chesapeake Bay is a highly dissipative system like the Georgia–Fuca system. Indeed, using a numerical tidal model validated against observed tidal heights and tidal currents in the Bay, Zhong and Li (2006) found that a total of 188 MW tidal energy is dissipated inside Chesapeake Bay, 60% of which is dissipated in the bottom boundary layer and 40% in four topographic hotspots characterized by sills, headlands and constrictions. Are these dissipative processes responsible for the low tidal amplification in the Bay? Will the dissipation be stronger or weaker if the frequency of offshore sea level fluctuations is lower than the tidal frequencies?

Sea level fluctuations in Chesapeake Bay encompass both tidal and subtidal frequencies. Subtidal variations in sea level have been linked to two primary mechanisms: local wind forcing on the Bay surface and remote long waves that enter at the Bay's mouth and propagate up the Bay (Garvine, 1985). In a series of papers examining subtidal water levels in the Bay, Wang and Elliot (1978) and Wang (1979a,b) found that the Bay exhibited a response at 2- to 5-day periods which was correlated to local wind forcing. They also found that the response at longer periods (10 days or more) was correlated to alongshore wind just outside the Bay's mouth, implying Ekman transport from the local shelf. Using classic quarter wavelength theory, Wang (1979a) estimated a resonant period of 1.46 days by taking the length of the Bay to be 280 km and the water depth 8.0 m, while Wang (1979b) got a slightly smaller value of 1.38 days by using different estimates of

the Bay's length and water depth. On the other hand, Chuang and Boicourt (1989) found seiche motions at the period of 1.6 days. These simple estimates of the resonant period are highly dependent on the choices for length and average depth. In this paper we use a numerical model to estimate the resonant period and the dissipation parameter Q for Chesapeake Bay and validate the model results against the observed amplitude gains and phase changes at the tidal and subtidal frequencies.

Chesapeake Bay is surrounded by low-lying lands populated by major cities. An accurate prediction of sea levels and clear understanding of resonant seiche motion is required not only for coastal-development planning but also for navigation as the Bay is a major US shipping route (Bosley and Hess, 2001). This need is made more urgent by the accentuated sea level rise in Mid-Atlantic estuaries. Global sea level has risen at a rate of $1.8 \pm 0.3 \text{ mm yr}^{-1}$ during the second half of the 20th century (Church et al., 2004) and is expected to increase at a substantially greater rate during the 21st century (Church et al., 2001). Due to the greater rate of absolute sea level rise in the middle latitudes of the Northwest Atlantic Ocean (Church et al., 2001) and land subsidence (Nerem et al., 1998), the sea level rise over Chesapeake Bay during the past 50 years is particularly large ($2.7\text{--}4.5 \text{ mm yr}^{-1}$, Zervas, 2001). A key question is then how this sea level rise will affect the tidal and subtidal sea level fluctuations inside the semi-enclosed Bay. Back of the envelope calculations suggest that sea level rise in Chesapeake Bay will likely shorten the resonant period and increase the tidal amplification. We will confirm this speculation by conducting a model run with higher sea level and examining the resonant response of Chesapeake Bay in a warming climate.

2. Observed tidal and subtidal sea level variability

Over 10 tide gauge stations are installed in Chesapeake Bay and have provided sea level measurements over the past several decades. These sea level data are archived at NOAA National Ocean Service's Center for Operational Oceanographic Products and Services which provides quality control (Bosley and Hess,

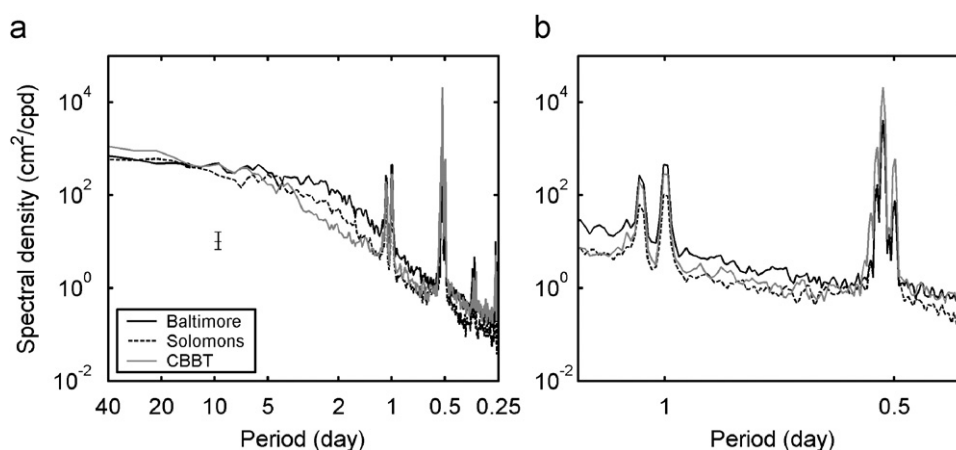


Fig. 2. (a) Energy spectra of water level fluctuations at three tidal gauge stations at 95% confidence intervals and (b) a zoom-in view for the tidal band.

2001). Both tides and winds contribute to sea level fluctuations in the Bay. In Fig. 2 we examine the frequency content of sea level fluctuations at three stations: CBBT, Solomons Island and Baltimore (see Fig. 1(a) for their locations). Station CBBT is near the Bay mouth and represents the lower Bay. Solomons Island is representative of the mid Bay. Although Baltimore is not located right at the Bay's head, it has been chosen to represent the upper Bay in the literature because the sea level data are deemed to be reliable and have a long record (cf., Wang, 1979a, b; Chuang and Boicourt, 1989; Bosley and Hess, 2001). The auto-spectral variance density functions are calculated using hourly sea level records spanning several years. The sea level records used for Baltimore and CBBT cover a 5-year period between 1994 and 1998, but the data record at the Solomons Island station is missing in 1994–95 and thus only covers 3 years between 1996 and 1998. Fig. 2(a) shows the highest peak in the semidiurnal tidal band and twin secondary peaks in the diurnal tidal band. Sea level fluctuations in the period between 2 and 10 days are associated with wind forcing. They are also high and comparable to those in the diurnal tidal band. The spectral density diagram shows that sea levels vary from the Bay's mouth to the head but this variation depends on the frequency or period of the oscillations. For example, sea level fluctuations in the frequency band of 2–10 days are lowest in the lower Bay and highest in the upper Bay. In contrast, the amplitude of the semidiurnal tide has the highest value at the Bay's mouth and lowest value at the head (Fig. 2(b)). The spectral density diagram also suggests that both tidal and subtidal sea level fluctuations are important in Chesapeake Bay. For example, the energy content in the subtidal band (period longer than 1.5 days) at the Baltimore station comprises 63% of the total energy.

We can get a clearer picture of the spatial tidal variability by examining the longitudinal variations of the M_2 and K_1 tidal amplitudes and phases. As shown by Zhong and Li (2006), M_2 and K_1 tides are the major tidal harmonics in the Bay. We select 11 tide gauge stations, occupying various points along the main stem of the Bay (see Fig. 1(a) for the locations) and collect their harmonic constants from the National Ocean Service's Center for Operational Oceanographic Products and Services. To show the amplitude and phase changes, we scale M_2 (K_1) amplitudes by their corresponding amplitudes at CBBT near the Bay's mouth and calculate the phases relative to the phases at the CBBT station, as shown in Fig. 3. M_2 and K_1 amplitudes decrease between the Bay's mouth and the Windmill Point station by about 50%. Windmill Point is located near the virtual amphidromes for both the M_2 and K_1 constituents (see Fig. 5). As shown in Zhong and Li (2006), the shallow lower Bay, including the headland in the southern tip of Delmarva Peninsula and the sill near Rappahannock shoals, are

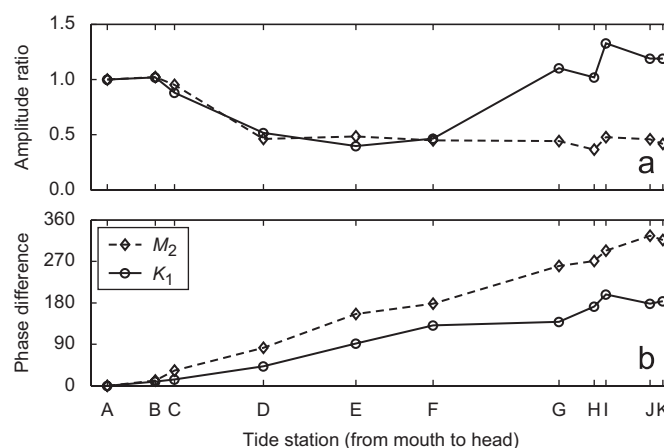


Fig. 3. Observed amplitude gain (a) and phase lag (b) of M_2 (diamond, dashed lines) and K_1 (circle, solid lines) harmonics at 11 tidal stations in Chesapeake Bay. Tidal amplitudes are scaled by those at the CBBT station and the phase lags are the differences from those at CBBT.

sites of high dissipation of tidal energy. Hence there are large reductions in tidal heights in the lower Bay. Between Windmill Point and the upper Bay station at Baltimore, the M_2 and K_1 amplitudes show different trends. The M_2 amplitude almost stays the same whereas the K_1 amplitude ratio increases steadily and reaches about 1.2 at Baltimore. Because Chesapeake Bay is relatively wide, the tide propagates as a Kelvin wave along the eastern shore, resulting in slightly higher tidal amplitudes there (Zhong and Li, 2006; Browne and Fisher, 1988). This east–west asymmetry is reflected in Fig. 3(a) as stations B, G, I and J have slightly different amplitude ratios than C, H, H and K, respectively.

Next, we look at the phase change for the M_2 and K_1 tidal components. As shown in Fig. 3(b), the phases of both constituents increase toward the head of Bay. The M_2 tide at Baltimore lags that at CBBT by about 320° . This shows that Chesapeake Bay is almost long enough to hold a complete M_2 wavelength inside the Bay. On the other hand, the K_1 tide at Baltimore lags that at CBBT by about 180° , indicating that the Bay can only accommodate one-half of its wavelength. The head-to-mouth differences for both tidal harmonics are significantly larger than the 90° phase lag expected at resonance, suggesting that resonant motion must occur at a subtidal frequency.

One can obtain a rough estimate of the resonance period according to the classic quarter wavelength theory $T = 4L/\sqrt{gh}$, where L is the length of a semi-enclosed Bay and h is the water

depth. Wang (1979a) chose 280 km and 8.0 m for these parameters while Wang (1979b) took them to be 270 km and 8.4 m. These two sets of values yield 1.46 and 1.38 days, respectively. Conversely, using observational data Wang and Elliott (1978) and Wang (1979a, b) consistently described the seiche period to be between 2 and 3 days, with 2.5 days being a common choice. Such simple estimates of resonant period are highly dependent on the choices for length and average depth of the Bay. In the next section, we shall use a numerical tidal model to obtain an accurate estimate of the resonance frequency in Chesapeake Bay.

3. Resonance diagram

We have configured the regional ocean modeling system (ROMS) for Chesapeake Bay (Li et al., 2005) and validated the model against a wide variety of observational data (Li et al., 2005, 2006, 2007; Zhong and Li, 2006). Fig. 1 shows the bathymetry and the orthogonal curvilinear coordinate system. Zhong and Li (2006) applied both 2D and 3D (barotropic and baroclinic) versions of the model to predict tidal heights and current ellipses in the Bay. For the sake of computational efficiency, we use the 2D model for the numerical experiments reported in this paper. For a detailed description of model configuration, the reader is referred to the Appendix.

To determine the resonance period, we carried out a set of numerical experiments with different sea level forcing at the open boundary. The sea level fluctuation is assumed to be sinusoidal with a single frequency. The amplitude of the sea level oscillation at the open boundary is fixed at 0.5 m, which is comparable to the amplitude of the dominant tide (M_2). There are two tidal gauge stations, Duck, VA and Wachepreague, VA, near the southern and northern ends of the open boundary, respectively. Harmonic analysis of tidal records shows that M_2 and K_1 tides at Duck, VA lead those at Wachepreague, VA by about 30° . Accordingly, a phase lag of 30° is specified between the southern and the northern ends of the open boundary though subsequent sensitivity tests demonstrated that 0° phase difference produced essentially the same resonance curves. We conducted numerical experiments by varying the forcing period over a broad range between 5 and 480 h. The model starts from a state of rest with the sea surface at the mean sea level. The model is run for 60 cycles and the last 20 cycles are selected for the time-series analysis.

As discussed earlier, we selected stations CBBT and Baltimore for calculating the amplitude ratio and phase difference. Fig. 4 shows the resonance diagram determined from the numerical experiments. The amplitude ratio reaches a peak around 2 days while the corresponding phase difference is 73° . (It is smaller than 90° because Baltimore lies south to the head of the Bay.) At very low frequencies, the Bay is short compared to the wavelength so that the sea levels in the Bay move synchronously and the amplitude gain is 1. At very high frequencies, wave energy is rapidly dissipated inside the Bay, resulting in a reduction in wave amplitude between the mouth and head. The amplitude gain at the resonance period is found to be 1.43.

Now we look at the phase difference between the estuary's head and mouth. Since Chesapeake Bay is long enough to hold a complete semidiurnal tidal wave at any time, the phase at Baltimore lags the phase at the mouth CBBT by about 310° . As the tidal period becomes longer, however, the Bay cannot hold a complete tidal wave anymore and the phase difference decreases. The longer the offshore forcing period is, the smaller the phase difference becomes. At diurnal frequencies the phase difference is about 170° as the Bay holds just half of a complete tidal wave.

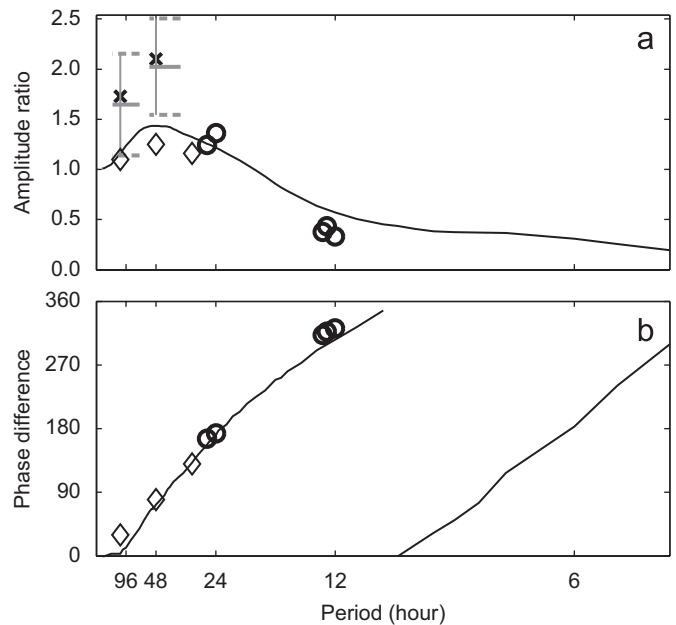


Fig. 4. Amplitude ratios (a) and phase differences (degrees, b) between the Baltimore station in the upper Bay and the CBBT station at the Bay mouth as a function of period (hours). Black solid lines are model predictions and circles are observed values for M_2 , N_2 , S_2 , K_1 , and O_1 . In (a), the heavy gray lines are the mean amplitude ratios calculated from the band-passed time series of observed water levels, while the dashed gray lines denote their standard deviations. Crosses (\times) are the amplitude ratios derived from the model simulations forced by both wind and tide. Diamonds are the results of model simulations where the offshore sea levels include both tidal and wind-driven sea level oscillations.

To validate the resonance diagram, we calculated the amplitude ratios and phase differences for the five major tidal constituents M_2 , S_2 , N_2 , K_1 and O_1 using the harmonic constants estimated from the sea level records at the tidal stations maintained by National Ocean Service's Center for Operational Oceanographic Products and Services. The model slightly over-predicted the amplitude gains at the semidiurnal frequencies and under-predicted those at the diurnal frequencies. The predicted phase changes agree almost perfectly with the observed values at the diurnal frequencies but are slightly below the semidiurnal values. Generally speaking, there is very good agreement between the predicted and observed amplitude gain and phase lag at the tidal frequencies.

It is instructive to plot the co-amplitude chart at the resonance frequency (see Fig. 5). If the Bay were a straight channel with constant water depth, the quarter wavelength theory would predict a node at the Bay's mouth and an anti-node at the Bay's head. Since the Bay has complex coastline and bathymetry, the node is not located at the Bay's mouth but at the entrance to the York River. Chuang and Boicourt (1989) recognized this and separated the Bay into two segments: a long, north–south portion covering the upper and middle Bay and an east–west portion covering the lower Bay. Simple analytic theory assuming constant water depth then gives a resonant frequency of 1.6 days. This is still shorter than the 2-day period obtained from our numerical model. However, one must be cautious when applying analytic models to real semi-enclosed seas. If we compare the node locations between different frequencies, we find that the node migrates south as the forcing frequency decreases: near Annapolis in the upper Bay at M_2 frequency (cf., Browne and Fisher, 1988; Zhong and Li, 2006), at the mouth of the Potomac River at K_1 frequency (which is also a node at about three-quarter of wave length from the head for M_2 tide, cf., Browne and Fisher, 1988;

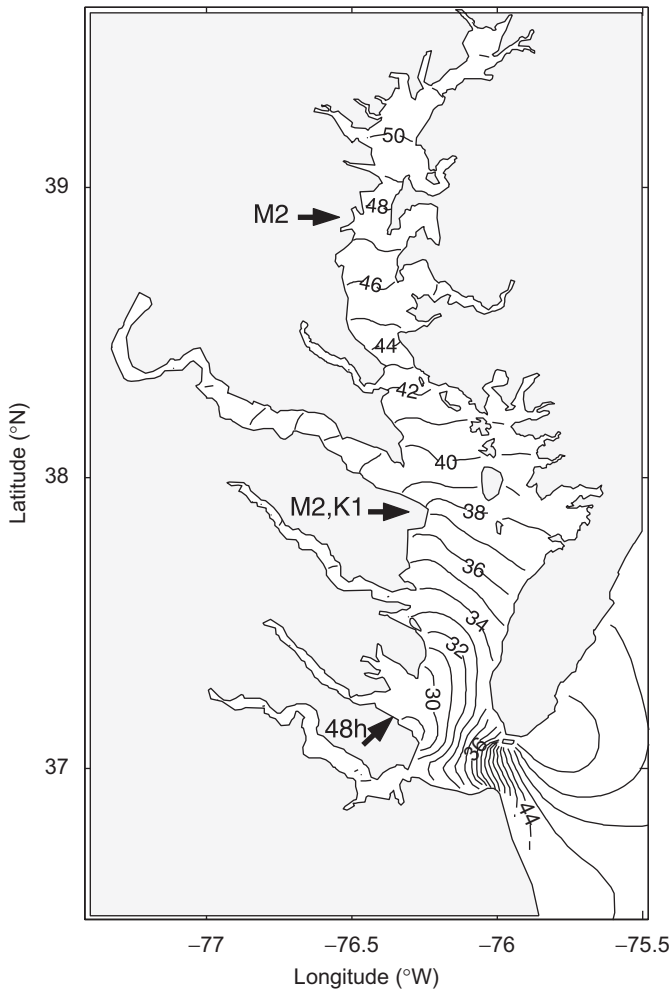


Fig. 5. Co-amplitude lines (in cm) at the resonance frequency. Three arrows mark the locations of virtual amphidromes for M2, K1 and 48-h period.

Zhong and Li, 2006), and at the mouth of the York River at the resonant frequency.

In the model runs discussed above, the sea level oscillation at the offshore open boundary is prescribed to be a sinusoid with a single frequency. This simple approach allows us to sweep through the frequency domain while keeping the amplitude of the oscillation constant. In reality, the sea level oscillation at the offshore boundary consists of tidal as well as non-tidal oscillations. Therefore, we conducted additional model runs in which the sea level at the open boundary is composed of the tidal oscillations (determined from the tidal model) and a non-tidal sinusoidal oscillation with an amplitude of 0.1 m. The amplitude gains and phase differences obtained from these model runs are included in Fig. 4 for comparison. The amplitude gains are somewhat smaller but show a peak at the same resonant (2-day) period. Bottom friction may be slightly stronger in the model runs that include the tidal components and this causes stronger damping of the wave motion in the Bay.

The amplitude gain of 1.43 is much smaller than the gains found in other semi-enclosed seas such as the Bay of Fundy. To understand this result, we calculated the resonance factor Q which is defined as the fraction of energy dissipated in a tidal/wave cycle, i.e., $Q = 2\pi N$, where N is the number of cycles required to dissipate the stored energy in the system. The total energy stored in Chesapeake Bay contains potential energy $E_p = (1/2)\int_S \rho g \eta^2 dS$ and kinetic energy $E_k = (1/2)\int_S \rho H(u^2 + v^2) dS$, where ρ is water density, H is water depth, η is the sea level

fluctuation, u and v are the depth-averaged horizontal velocity components, and the integral area S is the surface area of the Bay. The energy dissipation contains two parts. Most energy is dissipated through the bottom friction at the rate $\int_S \rho C_D (u^2 + v^2)^{3/2} dS$ (C_D is drag coefficient) while the rest is dissipated through horizontal diffusion at the rate $\int_S \rho H K_H (\nabla^2 u + \nabla^2 v) dS$ (∇^2 is the horizontal Laplacian operator and K_H the horizontal eddy viscosity). The total energy stored in the Bay at the resonance period of 48 h is found to be dissipated within 0.14 cycles, implying that the resonance factor Q equals 0.9. This value is much smaller than Q values for other coastal regions. For example, $Q = 18.8$ in the Gulf of California (Carbajal and Backhaus, 1998), $Q = 9.5$ in the north coast of British Columbia (Foreman et al., 1993) and $Q = 5.25$ in the Bay of Fundy (Garrett, 1972), respectively.

The low Q value indicates that Chesapeake Bay is highly dissipative. Indeed, Zhong and Li (2006) found that 188 MW of tidal energy is dissipated inside the Bay. Strong bottom friction together with isolated topographically induced dissipation cause rapid dissipation of tidal energy, thus providing effective impedance to the resonant response. The low Q value is consistent with the small amplitude gain shown in Fig. 4(a). In contrast, the amplitude gain is 20 in the Gulf of California (Carbajal and Backhaus, 1998), 17 in north coast of British Columbia (Foreman et al., 1993) where the Q values are considerably higher.

The small amplitude gain or the low Q value in Chesapeake Bay can also be obtained using the analytical model of Sutherland et al. (2005). If the Bay is approximated as a rectangle of length L and depth h , the amplitude gain can be obtained analytically from the linearized momentum and continuity equations. According to formula (13) in Sutherland et al. (2005), the amplitude gain at resonance is $A = (2\omega_0/\lambda)$, where ω_0 is the resonant frequency, $\lambda = ((C_D|u|)/h)$ is a linear friction coefficient which approximates the quadratic formula with C_D being the drag coefficient, and $|u|$ is the current magnitude. Using the relationship $Q = (\omega_0/\lambda)$, we estimated the linear friction coefficient $\lambda = 4.1 \times 10^{-5} \text{ ms}^{-1}$ for Chesapeake Bay.

These results can be put into a broad context regarding the responses of semi-enclosed seas to offshore sea level oscillations. In Table 1 we compare various parameters between several coastal systems. Chesapeake Bay, Juan de Fuca Strait and Strait of Georgia, have small amplitude gains and Q values but large bottom friction coefficients. In contrast, the north coast of British Columbia and Gulf of California have large amplitude gains and Q values but small friction coefficients. Long Island Sound and the

Table 1
Resonance comparison among the different coastal systems

Region	H (m)	L (km)	T (h)	A	Q	λ ($\times 10^{-5}$)
Chesapeake Bay	8.0	280	48	1.43	0.9	4.1
Bay of Fundy and Gulf of Maine	75	400	13.3		5.25	2.5
North coast of British Columbia	100	300	7.6	17	9.5	2.4
Gulf of California	650	1,000	14.57	20	18.8	0.64
Juan de Fuca Strait and Strait of Georgia	150	350	17–21	1.2	2	(4.2–5.1)
Long Island Sound	22	150	11–12	3–4		

Here H and L are the mean depth (m) and length (km) of the coastal system. T , A , Q are the resonant period (hour), amplitude gain and resonant factor, respectively. λ , the linear friction coefficient (ms^{-1}), is derived from Q and the resonant frequency (or period). T , A and Q (if available) values in other regions are inferred from previous studies: Bay of Fundy and Gulf of Maine from Garrett (1972); north coast of British Columbia from Foreman et al. (1993); Gulf of California from Carbajal and Backhaus (1998); Juan de Fuca Strait and Strait of Georgia from Sutherland et al. (2005) and Long Island Sound from Wong (1990).

Bay of Fundy and Gulf of Maine have intermediate values of amplitude gains, Q values and bottom friction coefficients. While Chesapeake Bay and the Fuca–Georgia system have resonant periods far away from the tidal periods, it is not immediately clear which factor controls the resonance in the other four coastal systems. The Gulf of California and north coast of British Columbia have the highest gains but the distances between their natural resonant period and tidal periods are longer than those in Long Island Sound and the Bay of Fundy–Gulf of Maine. A closer examination shows that the friction coefficient is smaller in Gulf of California and north coast of British Columbia. Therefore, it appears that both the magnitude of the bottom friction and the distance between the natural resonance frequency and the forcing frequency (primarily tidal frequencies) play important roles in controlling the resonance response in semi-enclosed seas.

In addition to examining the dissipation parameter at the resonance frequency, we calculated N and Q for the semidiurnal (period 12 h) and diurnal (period 24 h) tides and the subtidal period of 96 h. The pairs of N and Q are 0.35/2.2, 0.21/1.3, 0.26/1.7 at $T = 12, 24$ and 96 h, respectively. We can also calculate the friction coefficient at these frequencies. The friction coefficients for periods of 12, 24, 48 and 96 h are 6.6×10^{-5} , 5.5×10^{-5} , 4.1×10^{-5} and $2.2 \times 10^{-5} \text{ ms}^{-1}$, respectively. Chesapeake Bay experiences less damping at the resonance frequency than at the tidal frequencies, thus leading to relatively large amplification in the wave amplitude from the Bay's mouth to the head. At low frequencies, however, the Bay is short compared to the wavelength so that sea levels inside the Bay move synchronously and the amplitude gain is 1.

To better understand dissipation at different forcing frequencies, we map out the spatial distribution of energy dissipation inside the Bay at $T = 12, 24, 48$ and 96 h. The distribution of the energy dissipation rate at 12-h forcing (Fig. 6(a)) is very similar to that obtained from the 3D baroclinic model for the M_2 tide (Fig. 11c in Zhong and Li, 2006). There are four topographic hotspots of high-energy dissipation: two in the lower Bay (the Bay mouth region around the headland of Delmarva Peninsula and the region near the Rappahannock Sill) and two in the upper Bay (one constriction near the Bay Bridge and another north of Baltimore). The energy dissipation at 24-h forcing (Fig. 6(b)) bears some similarity to that at 12-h forcing. Three hotspots (two in the lower Bay and one at the constriction near the Bay Bridge) still exist at the same locations. However, a new dissipation hotspot appears near the mouth of Patuxent River while the hotspot near Baltimore disappears. At the resonance period of 48-h the spatial pattern of energy dissipation rate looks very different (Fig. 6(c)). The high dissipation regions in the middle and upper Bay are

mostly gone. Most of the energy is dissipated in the lower Bay. At the subtidal period of 96 h (Fig. 6(d)), energy dissipation is mostly concentrated near the Bay's mouth and is smaller than that at the resonant frequency. To summarize the comparison, we find that high-energy regions retreat towards the Bay's mouth as the forcing frequency is reduced. This change in the spatial distribution of energy dissipation may explain the gradual increase of the amplitude gain from the tidal frequency band to the resonant band in the resonance diagram (Fig. 4(a)). At very low forcing frequencies such as 96-h period in Fig. 6(d), the dissipation is reduced further (the total energy dissipation at 96-h period is only one-third of that at the resonant period). However, the Bay behaves like a water tank that is gradually filled with shelf water, so that the amplitude gain is nearly identical to 1.

4. Local and remote wind forcing of sea level oscillations

Our calculations identified a resonance period of 2 days, which is longer than the major tidal periods. As discussed in Section 2 and shown in Fig. 2, sea level fluctuations in Chesapeake Bay contain significant non-tidal components associated with meteorological forcing. We can use these subtidal sea level data to test the resonance diagram at the resonant and other subtidal frequencies. Sea level records at CBBT, Solomons Island and Baltimore will be used in the analysis. To assist the interpretation of the subtidal sea level variability, we also examine the wind data at two stations: station PRN in mid Bay which is representative of local wind forcing; station NIA near the Bay mouth which is representative of remote wind forcing. In order to extract the contents of the data series near the resonance frequency, we apply a Butterworth band-pass filter whose cutoff periods are set at 34 and 54 h to the sea level and wind time series.

The band-passed wind and sea levels over a 20-day period (Fig. 7) clearly show that the sea level fluctuations increase between the mouth and head of the Bay. To calculate the amplitude gain between Baltimore and CBBT, we used the standard deviation of each time series. Although Fig. 7 only covers a 20-day period, we examined the amplitude gain between 1994 and 1998 and calculated an amplitude ratio for each month of the 5-year period. These amplitude ratios were then used to calculate the mean and standard deviation, which are plotted in Fig. 4(a) for comparison with the model prediction. The amplitude gain obtained from the resonance calculations falls below the observed range and is 29% smaller than the mean amplitude gain of 2.0 estimated from the sea level observations.

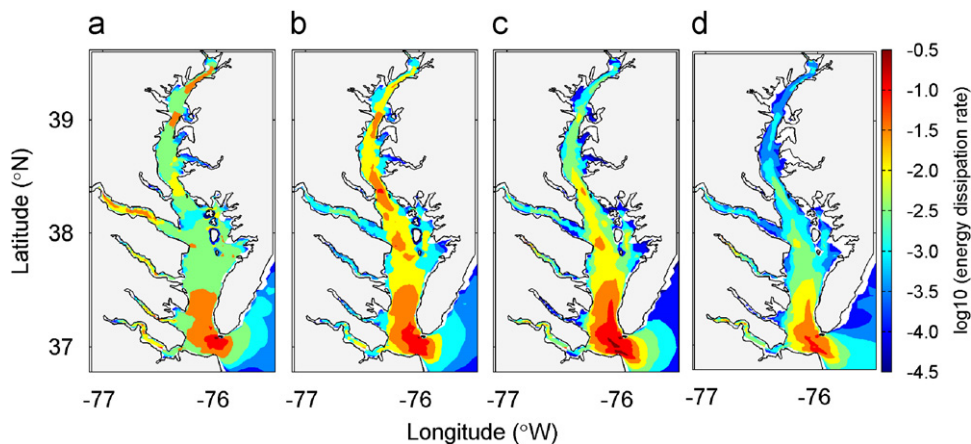


Fig. 6. Distributions of the energy dissipation rate in Chesapeake Bay for offshore forcing at the periods 12 h (a), 24 h (b), 48 h (c) and 96 h (d).

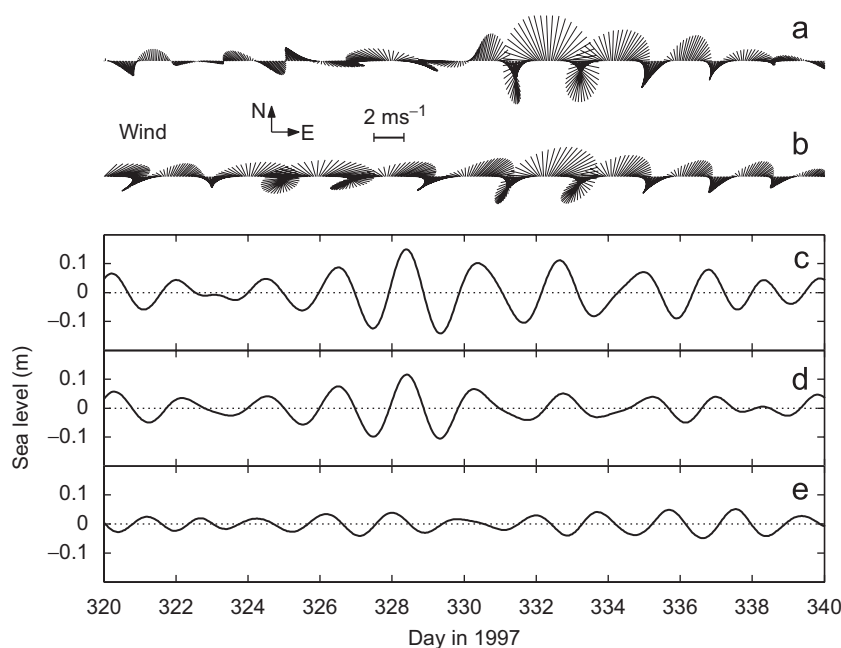


Fig. 7. Band-passed (cutoff periods are 34 and 54 h) time series of the observed wind vector at the PRN station in the middle Bay (a) and the NIA station nearby the Bay mouth (b), band-passed observed water level fluctuations at Baltimore (c), Solomons Island (d) and CBBT (e) over a 20-day period.

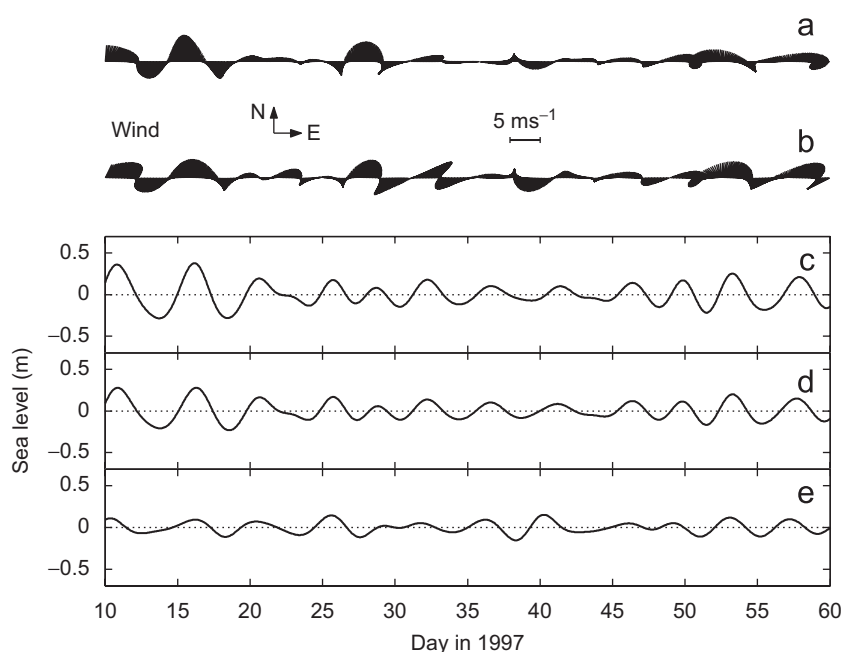


Fig. 8. Band-passed (cutoff periods are 3 and 7 days) observed wind vectors at the stations of PRN (a) and NIA (b), and band-passed observed water level fluctuations at Baltimore (c), Solomons Island (d) and CBBT (e) over a 50-day period.

The discrepancy between the observed and predicted amplitude gains is likely due to the neglect of local wind forcing in the resonance calculations, as suggested in previous papers. Wang and Elliot (1978) found that water levels co-vary with local winds in Chesapeake Bay. Using simple analytic models, Garvine (1985) and Wong and Moses-Hall (1998) studied an idealized estuary's response to local and remote wind effects. Their results suggest that both remote and local wind effects can generate resonant motion in the estuary if the wind frequency matches the natural resonance frequency of the estuary.

To examine if the local wind is indeed responsible for the observed amplified response, we have added wind forcing to the model. The wind blows in the north–south direction, oscillates at the resonant frequency, is spatially uniform and has the peak stress magnitude of 0.03 N m^{-2} (corresponding to the band-passed wind speed shown in Fig. 7(a)). At the offshore open boundary, the sea level oscillation consists of the tidal constituents as well as a non-tidal oscillation of 0.1 m amplitude at a 2-day period. The predicted sea levels at Baltimore and CBBT are band-passed to calculate the amplitude gain. The non-tidal sea levels

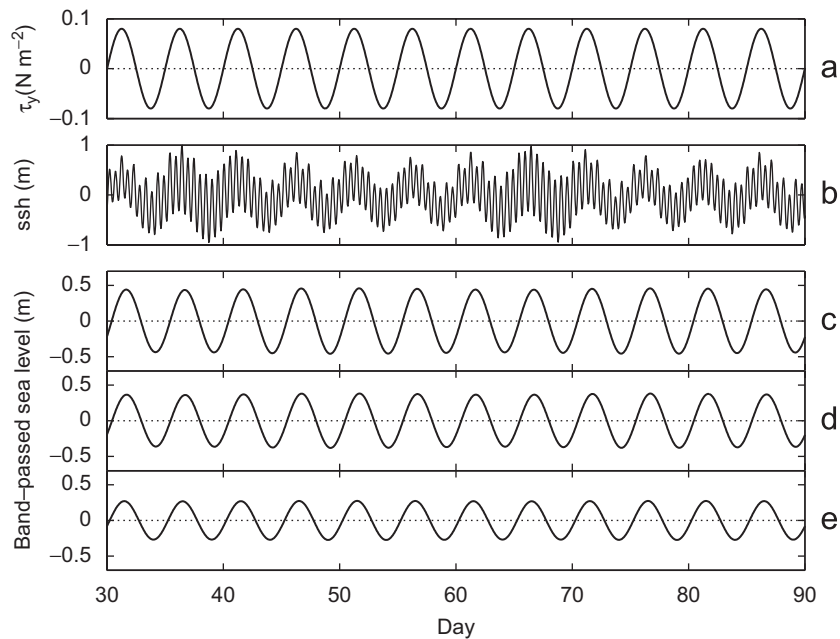


Fig. 9. Time series of the north-south wind stress component (a), offshore sea level fluctuations (b), and model-predicted sea level oscillations at Baltimore (c), Solomons Island (d) and CBBT (e), respectively.

can also be calculated as the difference between the total sea level and tidal components. The latter method gives identical non-tidal sea levels as those obtained from the band-passed time series. The amplitude gain between Baltimore and CBBT is now estimated to be 2.1, which is almost identical to the value of 2.0 estimated from the observed sea level records in the resonance frequency band of 34–54 h (Fig. 4(a)).

Wang (1979a) found that winds also generated large sea level fluctuations at the frequency band of 3–7 days. Indeed, we found large sea level fluctuations at this frequency band from the 5-year sea level records discussed earlier (Fig. 8). The amplitude gain between Baltimore and CBBT is calculated and shown in Fig. 4(a). Again the observed amplitude gain is larger than that predicted from the resonance calculations. The mismatch is likely caused by the neglect of local wind forcing. To verify this, we forced the numerical model with a spatially uniform wind field oriented in the north-south direction and oscillating at 5-day period with the peak magnitude of 0.08 N m^{-2} (corresponding to the band-passed wind speed in Fig. 8(a)), as shown in Fig. 9(a). The offshore sea levels include the tidal constituents as well as a non-tidal oscillation with 0.3 m amplitude and 5-day period (see Fig. 9(b)). Fig. 9(c–e) shows the band-passed time series of sea levels at Baltimore, Solomons Island and CBBT, respectively. The predicted amplitude gain between Baltimore and CBBT is 1.73 with the inclusion of local wind forcing (see Fig. 4(a)), confirming that the local wind forcing amplifies the sea level variability inside the Bay. The predicted gain is only 4% larger than the mean gain inferred from the observed sea level fluctuations at the frequency band of 3–7 days. In summary, our model calculations have shown that both the local and remote wind forcing contribute to amplified sea level response in Chesapeake Bay at subtidal frequencies.

5. Conclusion

Using a numerical model, we have obtained a resonance diagram for Chesapeake Bay and validated the model predictions against observed sea level fluctuations at tidal and subtidal

frequencies. The resonance period is found to be 2 days. The amplitude gain between CBBT and Baltimore is 1.43 while the phase change between the two stations is 73° . Due to its shallowness and long resonance period, Chesapeake Bay experiences more friction at the resonant frequency than other coastal systems. It has a much smaller amplitude gain than the Bay of Fundy and Gulf of Maine, the north coast of British Columbia and the Gulf of California. The modest gain in Chesapeake Bay is consistent with its low Q value of 0.9. This suggests that Chesapeake Bay is a highly dissipative system preventing strong resonant response.

Both local winds and remote winds can generate sea level oscillations inside Chesapeake Bay. As shown in the resonance diagram, coastal sea level oscillations driven by the remote winds at the resonant period only lead to about 50% amplification at the Bay's head. An analysis of sea level time series in the resonant band reveals additional amplification which is found to be caused by the local wind forcing. The combined local and remote wind forcing thus result in approximately 100% amplification of sea level oscillations between the Bay's mouth and head. Although this amplification is small compared to other coastal systems, it still poses serious concerns to the low-lying land surrounding Chesapeake Bay.

Though global sea level rise largely due to a combination of a warmer ocean and melting of the Greenland and Antarctic ice caps will, in itself, cause many flooding problems for communities and infrastructure around Chesapeake Bay, it is important to note that this rise will also change the resonance characteristics of the Bay. In particular, given its relative shallowness, sea level rise can be expected to have a much larger effect on resonance in Chesapeake than in many other bays whose average depth is larger. An increase in the average depth will cause a decrease in the resonant period, which in this case will make it closer to that for the diurnal tides. As shown in Fig. 10, given a hypothetical sea level rise of 1 m, the resonant period moves toward the diurnal tidal band and the amplitude gain also increases due to friction reduction. Though model calculations that incorporate a changing coastline are needed to determine these changing tidal patterns more precisely, a larger tidal range that will further exacerbate flooding

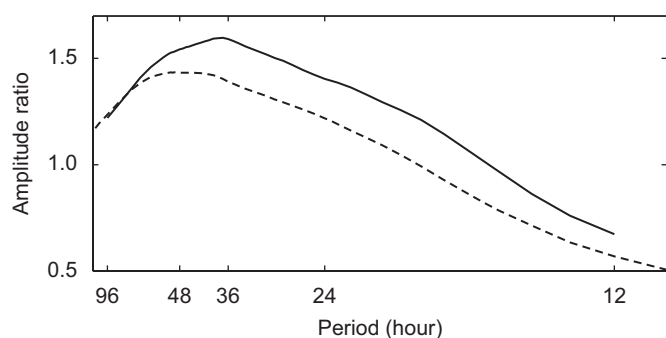


Fig. 10. Resonance response diagram of Chesapeake Bay under current sea level (dashed line) and 1-m sea level rise (solid line) conditions.

problems can generally be expected. Studies to monitor the consequences of these future resonance changes are therefore warranted.

Acknowledgments

We thank NOAA for providing sea level data at the tidal gauges in Chesapeake Bay. This work is supported by grants from NOAA. This is UMCES contribution number 4016.

Appendix A. The numerical model configuration

The regional ocean modeling system (ROMS) has been configured for Chesapeake Bay. The model bathymetry, shown in Fig. 1(a), is extracted from high-resolution Coastal Relief Model data archived at NOAA's National Geophysical Data Center. The model domain includes the main stem of the Bay, eight major tributaries, and a piece of the coastal ocean (Fig. 1). The horizontal coordinate system is orthogonal curvilinear to follow the general orientation of the deep channel and the coastline of the main stem. The grid size is less than 1 km in the cross-channel direction and 2–3 km in the along-channel direction. The total number of grid points is 120 × 80.

The bottom stress is parameterized as a quadratic function of the depth-averaged current. To account for the effect of the water depth, the drag coefficient C_D is prescribed as $C_D = gC^{-2}$, $C = h^\alpha n^{-1}$ in which h is the undisturbed water depth, C is the Chezy coefficient, and constant parameters α , n are chosen to be 1/6 and 0.02, respectively (cf., Spitz and Klinck, 1998; Daily and Harleman, 1966). This empirical formula links the flow resistance factor C to the drag coefficient. In our model, the minimum water depth is set to be 2.5 m and the corresponding drag coefficient is 0.0029. The open-ocean boundary condition consists of a Chapman condition for surface elevation and a Flather condition for barotropic velocity. At the upstream boundary in each tributary, the incoming current, uniform on each inflow cross section, is regulated by freshwater discharge rate, and the Chapman radiation condition is used to filter out the outgoing tidal waves. In this paper the freshwater flow rates are kept constant during the model integrations. The total flow rate is fixed at the long-term average of $1500 \text{ m}^3 \text{ s}^{-1}$: 50% is allocated to the Susquehanna River, 20% to the Potomac River, 15% to the James River while the

remaining 15% is divided evenly among the five smaller tributaries (Choptank, Patapsco, Patuxent, Rappahannock and York) (cf., Li and Zhong, 2008). Horizontal eddy viscosity is set to $1 \text{ m}^2 \text{ s}^{-1}$. The model starts from a state of rest with the sea surface at the mean sea level. The model has a time step of 15 s.

References

- Bosley, K.T., Hess, K.W., 2001. Comparison of statistical and model-based hindcasts of subtidal water levels in Chesapeake Bay. *Journal of Geophysical Research* 106 (C8), 16,869–16,885.
- Browne, D.R., Fisher, C.W., 1988. Tide and tidal currents in the Chesapeake Bay. NOAA Technical Report NOS OMA 3.
- Carbajal, N., Backhaus, J.O., 1998. Simulation of tides, residual flow and energy budget in the Gulf of California. *Oceanologica Acta* 21, 429–446.
- Chuang, W.-S., Boicourt, W.C., 1989. Resonant seiche motion in the Chesapeake Bay. *Journal of Geophysical Research* 94, 2105–2110.
- Church, J.A., Gregory, J.M., Huybrechts, P., Kuhn, M., Lambeck, K., Nhuon, M.T., Qin, D., Woodworth, P.L., 2001. Changes in sea level. In: Houghton, J.T., Ding, Y., Griggs, D.J., Noguer, M., van der Linden, P.J., Dai, X., Maskell, K., Johnson, C.A. (Eds.), *Climate change 2001: The Scientific Basis, Contribution of Working Group I to the Third Assessment Report of the Intergovernmental Panel on Climate Change*. Cambridge University Press, Cambridge, p. 881.
- Church, J., White, N., Coleman, R., Lambeck, K., Mitrovica, J., 2004. Estimates of the regional distribution of sea level rise over the 1950–2000 period. *Journal of Climate* 17, 2609–2625.
- Daily, J.W., Harleman, D.R.F., 1966. *Fluid Dynamics*. Addison-Wesley Publishing Company, Inc., Reading, MA, pp. 297–298.
- Foreman, M.G.G., Henry, R.F., Walters, R.A., Ballantyne, V.A., 1993. A finite element model for tides and resonance along the north coast of British Columbia. *Journal of Geophysical Research* 98 (C2), 2509–2531.
- Garrett, C., 1972. Tidal resonance in the Bay of Fundy and Gulf of Maine. *Nature* 238, 441–443.
- Garvine, R.W., 1985. A simple model of estuarine subtidal fluctuations forced by local and remote wind stress. *Journal of Geophysical Research* 90, 11,945–11,948.
- Li, M., Zhong, L., 2008. Flood–ebb and spring–neap variations of mixing, stratification and circulation in Chesapeake Bay. *Continental Shelf Research*. in press, doi:10.1016/j.csr.2007.06.012.
- Li, M., Zhong, L., Boicourt, W.C., 2005. Simulations of Chesapeake Bay estuary: sensitivity to turbulence mixing parameterizations and comparison with observations. *Journal of Geophysical Research* 110, C12004.
- Li, M., Zhong, L., Boicourt, W.C., Zhang, S., Zhang, D.-L., 2006. Hurricane-induced storm surges, currents and destratification in a semi-enclosed bay. *Geophysical Research Letters* 33, L02604.
- Li, M., Zhong, L., Boicourt, W.C., Zhang, S., Zhang, D.-L., 2007. Hurricane-induced destratification and restratification in a partially-mixed estuary. *Journal of Marine Research* 65, 169–192.
- Nerem, R.S., van Dam, T.M., Schenewerk, M.S., 1998. Chesapeake Bay subsidence monitored as wetlands loss continues. *EOS Transactions, AGU* 79 (12), 149 pp. 156–157.
- Spitz, Y.H., Klinck, J.M., 1998. Estimate of bottom and surface stress during a spring–neap tide cycle by dynamic assimilation of tide gauge observations in the Chesapeake Bay. *Journal of Geophysical Research* 103, 12761–12782.
- Sutherland, G., Garrett, C., Foreman, M., 2005. Tidal resonance in Juan de Fuca Strait and the Strait of Georgia. *Journal of Physical Oceanography* 35, 1279–1286.
- Wang, D.-P., 1979a. Subtidal sea level variations in the Chesapeake Bay and relation to atmospheric forcing. *Journal of Physical Oceanography* 9, 413–421.
- Wang, D.-P., 1979b. Wind-driven circulation in the Chesapeake Bay, winter 1975. *Journal of Physical Oceanography* 9, 564–572.
- Wang, D.-P., Elliot, A.J., 1978. Non-tidal variability in the Chesapeake Bay and Potomac River: evidence for non-local forcing. *Journal of Physical Oceanography* 8, 225–232.
- Wong, K.-C., 1990. Sea level variability in Long Island Sound. *Estuaries* 13 (4), 362–372.
- Wong, K.-C., Moses-Hall, J.E., 1998. On the relative importance of the remote and local wind effects to a subtidal variability on a coastal plain estuary. *Journal of Geophysical Research* 103, 18393–18404.
- Zervas, C., 2001. Sea level variations of the United States 1854–1999. National Oceanic and Atmospheric Administration Technical Report NOS CO-OPS 36. Silver Spring, MD, USA.
- Zhong, L., Li, M., 2006. Tidal energy fluxes and dissipation in the Chesapeake Bay. *Continental Shelf Research* 26, 752–770.